Journal of Molecular Cell Biology (2022), 14(10), mjac068 https://doi.org/10.1093/jmcb/mjac068
Published online December 9, 2022

Article

Type IV collagen α5 chain promotes luminal breast cancer progression through c-Myc-driven glycolysis

Yuexin Wu[1,2,3,†], Xiangming Liu[1,2,†], Yue Zhu[1,2], Yuemei Qiao[1], Yuan Gao[1], Jianfeng Chen[1,4], and Gaoxiang Ge[1,4,*]

[1] State Key Laboratory of Cell Biology, Shanghai Institute of Biochemistry and Cell Biology, Center for Excellence in Molecular Cell Science, Chinese Academy of Sciences, Shanghai 200031, China
[2] University of Chinese Academy of Sciences, Beijing 100049, China
[3] Affiliated Cancer Hospital of Zhengzhou University & Henan Cancer Hospital, Zhengzhou 450008, China
[4] Key Laboratory of Systems Health Science of Zhejiang Province, School of Life Science, Hangzhou Institute for Advanced Study, University of Chinese Academy of Sciences, Hangzhou 310024, China
[†] These authors contributed equally to this work.
* Correspondence to: Gaoxiang Ge, E-mail: gxge@sibcb.ac.cn

Edited by Hua Lu

Cancer cell metabolism reprogramming is one of the hallmarks of cancer. Cancer cells preferentially utilize aerobic glycolysis, which is regulated by activated oncogenes and the tumor microenvironment. Extracellular matrix (ECM) in the tumor microenvironment, including the basement membranes (BMs), is dynamically remodeled. However, whether and how ECM regulates tumor glycolysis is largely unknown. We show that type IV collagens, components of BMs essential for the tissue integrity and proper function, are differentially expressed in breast cancer subtypes that α5 chain (α5(IV)) is preferentially expressed in the luminal-type breast cancer and is regulated by estrogen receptor-α. α5(IV) is indispensable for luminal breast cancer development. Ablation of α5(IV) significantly reduces the growth of luminal-type breast cancer cells and impedes the development of luminal-type breast cancer. Impaired cell growth and tumor development capability of α5(IV)-ablated luminal breast cancer cells is attributed to the reduced expression of glucose transporter and glycolytic enzymes and impaired glycolysis in luminal breast cancer cells. Non-integrin collagen receptor discoidin domain receptor-1 (DDR1) expression and p38 mitogen-activated protein kinase activation are attenuated in α5(IV)-ablated luminal breast cancer cells, resulting in reduced c-Myc oncogene expression and phosphorylation. Ectopic expression of constitutively active DDR1 or c-Myc restores the expression of glucose transporter and glycolytic enzymes, and thereafter restores aerobic glycolysis, cell proliferation, and tumor growth of luminal breast cancer. Thus, type IV collagen α5 chain is a luminal-type breast cancer-specific microenvironmental regulator modulating cancer cell metabolism.

Keywords: luminal breast cancer, basement membrane, type IV collagen, COL4A5, glycolysis, Myc

Introduction

Cancer cell metabolism reprogramming is one of the hallmarks of cancer (Hanahan and Weinberg, 2011). Cancer cells preferentially utilize aerobic glycolysis to provide cancer cells rapid energy production and substrates for biosynthetic pathways (Ward and Thompson, 2012). Cancer cell glycolysis is regulated by activated oncogenes, e.g. Myc (Hsieh et al., 2015), and mutant tumor suppressors, e.g. p53 (Liu et al., 2019). Cancer cell glycolysis is also regulated by the tumor microenvironment. The hypoxic microenvironment increases protein levels of the HIF1α and HIF2α transcription factors, which in turn upregulate the expression of glucose transporters and glycolytic enzymes (Denko, 2008). Cytokines, e.g. IL-6, secreted by tumor-associated macrophages (Zhang et al., 2018), myeloid-derived

Received May 28, 2022. Revised September 27, 2022. Accepted December 7, 2022.

suppressor cells (Li et al., 2018), or cancer-associated fibroblasts (Bertero et al., 2019) in the tumor microenvironment promote cancer cell glycolysis and metabolism.

Extracellular matrix (ECM), including collagens, glycoproteins, and proteoglycans (Hynes and Naba, 2012; Naba et al., 2012), is dynamically remodeled in the tumor microenvironment. Basement membranes (BMs) are specialized ECMs underneath epithelial cells and cancer cells (Kalluri, 2003; Pozzi et al., 2017). Type IV collagens and laminins are the core components of BMs building the framework of BMs (Pozzi et al., 2017), in which type IV collagen networks are essential for the maintenance of BM structure (Poschl et al., 2004). In mammals, there are six highly homologous type IV collagen α chains (α1(IV)–α6(IV)) (Zhou et al., 1994) forming heterotrimeric major type IV collagen α1α1α2(IV) and minor type IV collagens α3α4α5(IV) and α5α5α6(IV) (Butkowski et al., 1989; Gunwar et al., 1998; Boutaud et al., 2000; Borza et al., 2001). Major and minor type IV collagen subtypes are temporospatially expressed and remodeled (Wu and Ge, 2019; Wu et al., 2021) and exert subtype-specific functions through integrin and non-integrin receptors (Xiao et al., 2015; Wu et al., 2021). α5(IV) supports lung cancer progression by promoting lung cancer cell proliferation and tumor angiogenesis through the non-integrin collagen receptor discoidin domain receptor-1 (DDR1) (Xiao et al., 2015). Thus, ECM proteins not only provide cells with structural support but also actively participated in regulating cancer cell survival, proliferation, and tumorigenesis (Pietras and Ostman, 2010). However, it is largely unknown whether and how ECM regulates cancer cell metabolism.

In the present study, we demonstrate that α5(IV) is preferentially expressed in luminal-type breast cancer and is indispensable for luminal breast cancer development. α5(IV) promotes cancer cell glycolysis through the DDR1–p38 mitogen-activated protein kinase (MAPK)–c-Myc signaling axis and thus supports breast cancer cell proliferation and luminal breast cancer progression.

Results

α5(IV) collagen is expressed in luminal breast cancer

BMs are specialized ECMs underneath epithelial cells, endothelial cells, peripheral nerve axons, adipocytes, and muscle cells (Kalluri, 2003; Pozzi et al., 2017). BMs are highly complex structures with tissue-specific protein composition (Randles et al., 2017). Breast cancer is highly heterogeneous encompassing five distinctive breast cancer subsets, i.e. basal-like, ERBB2, luminal A, luminal B, and normal breast-like subtypes, which exhibit diverse clinical features and outcomes. We first asked whether breast cancer subtypes possess subtype-specific BM composition. Correlation analyses of the expression of core components of BMs revealed two groups of co-expressed BM components in the Netherlands Cancer Institute (NKI) breast cancer cohort (Figure 1A). One group highly correlates with the signatures of luminal A and normal breast-like subtypes, whereas the second group highly correlates with the signatures of basal-like, ERBB2, and luminal B subtypes (Figure 1A), suggesting that breast cancer may possess subtype-specific BMs. In particular, minor type IV collagen *COL4A5* and major type IV collagen *COL4A1*/*COL4A2* correlate with luminal A/normal breast-like and basal-like/ERBB2/luminal B breast cancer subtype signatures, respectively (Figure 1A). Minor type IV collagen *COL4A5* expression highly correlates with the expression of *ESR1* and *GATA3*, two key transcription factors in luminal-type breast cancer (Figure 1A). Consistently, *COL4A5* expression is higher in the luminal A type, compared to that in the basal-like type (Figure 1B), and is significantly higher in the estrogen receptor-α (ERα)-positive (ER+) breast cancer, compared to that in the ERα-negative (ER–) breast cancer (Figure 1C). *COL4A5* is also highly expressed in ERα-positive luminal-type breast cancer in a second breast cancer cohort (Supplementary Figure S1). Consistent with the subtype-specific *COL4A5* expression in breast cancer tumors, both mRNA (Figure 1D) and protein (Figure 1E and F) levels of *COL4A5* were significantly higher in ERα-positive luminal-type breast cancer cell lines. Knockdown of ERα in luminal-type breast cancer cell lines significantly reduced α5(IV) collagen expression (Supplementary Figure S2A).

α5(IV) collagen is essential to luminal breast cancer cell proliferation

Knockdown of ERα significantly reduced cell proliferation (Supplementary Figure S2B and C). We next investigated whether the downstream α5(IV) collagen regulates luminal breast cancer cell proliferation. Knockdown of α5(IV) collagen significantly impaired the cell proliferation of MCF-7 and T-47D cells (Figure 1G). 5-ethynyl-2′-deoxyuridine (EdU) incorporation assay further indicated the reduced DNA synthesis in α5(IV) collagen-knockdown MCF-7 and T-47D cells (Figure 1H). ERα-positive *MMTV-PyVT* murine mammary tumors expressed α5(IV) collagen, which was not expressed by ERα-negative basal type *MMTV-Wnt1* murine mammary tumors (Supplementary Figure S3A and B). To study the functions of α5(IV) collagen in breast cancer progression *in vivo*, *MMTV-PyVT* mice were crossed with *Col4a5*$^{f/f}$;*Krt8-CreERT2* mice to inducibly knock out α5(IV) collagen in luminal breast cancer cells (Figure 2; Supplementary Figure S3C). Despite ablation of α5(IV) collagen in keratin 8-positive luminal mammary epithelial cells did not affect the multiplicity of mammary tumors (Figure 2A), ablation of α5(IV) collagen significantly reduced the growth rate of *PyVT* tumors (Figure 2B) with prolonged survival after tumor onset (Figure 2C). Consistent with the reduced proliferation of MCF-7 and T-47D cells upon α5(IV) collagen knockdown (Figure 1G and H), ablation of α5(IV) collagen significantly reduced the numbers of Ki67-positive cells in *PyVT* tumors (Figure 2D and E). Isolated α5(IV) collagen-ablated (knockout, KO) *PyVT* tumor cells grew much more slowly than the wild-type (WT) *PyVT* tumor cells with much less EdU incorporation (Figure 2F and G). KO *PyVT* cells had impaired capability in developing xenograft tumors, with delayed tumor onset and reduced xenograft tumor growth (Figure 2H and I). These data collectively indicated that α5(IV) collagen expressed by luminal breast cancer cells promoted luminal breast cancer cell proliferation and tumor progression.

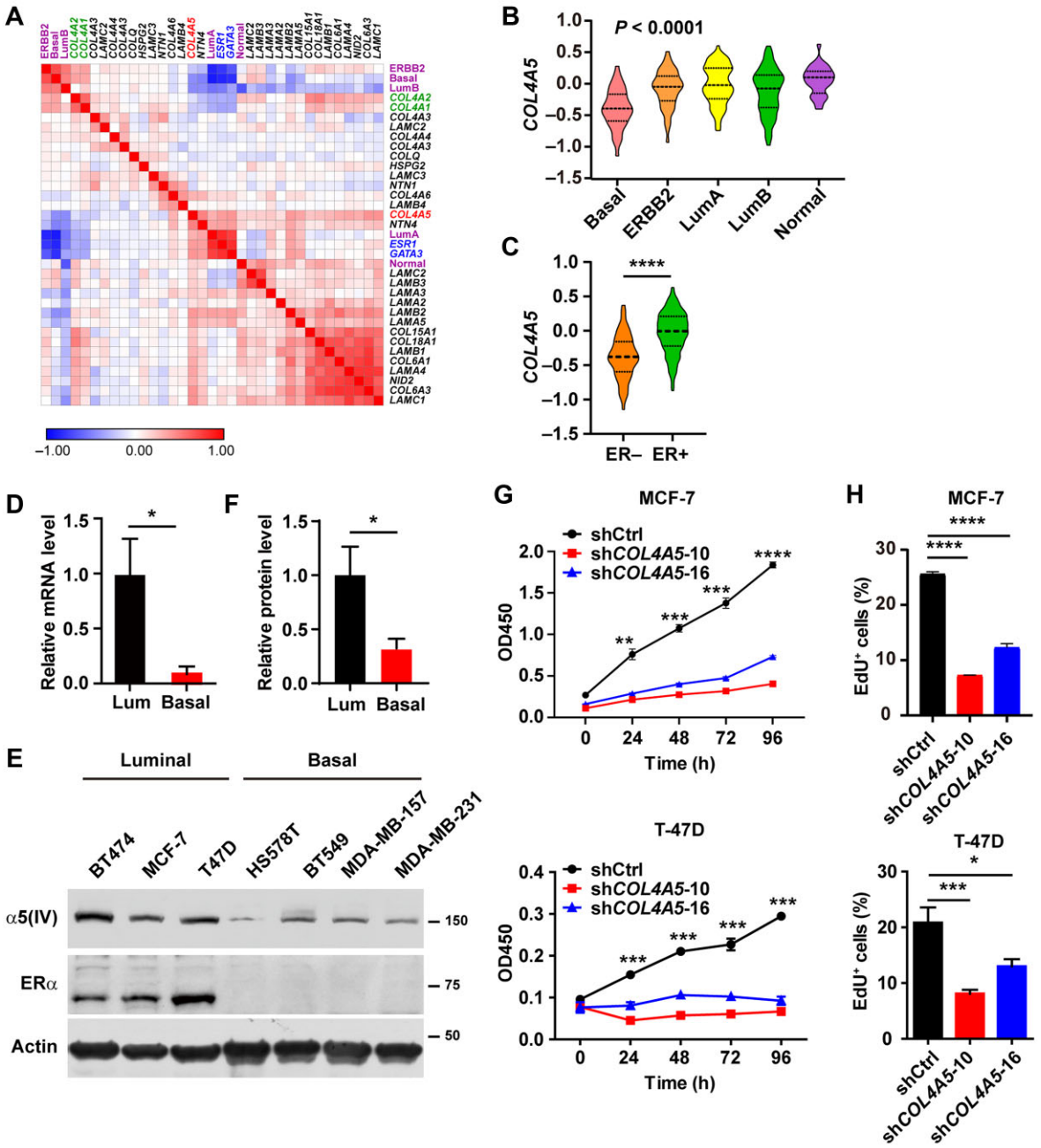

Figure 1 α5(IV) collagen is expressed in luminal breast cancer and regulates breast cancer cell proliferation. (**A**) Heatmap of Pearson's correlation coefficient of BM components (green font: major α1(IV) and α2(IV); red font: minor α5(IV)), breast cancer subtype scores (purple font), and luminal breast cancer key transcription factors ERα and GATA-3 (blue font) in the NKI cohort. (**B**) Expression of *COL4A5* in breast cancer subtypes in the NKI cohort. (**C**) Expression of *COL4A5* in ERα-negative (ER–) and ERα-positive (ER+) breast cancer in the NKI cohort. (**D**) Relative mRNA levels of *COL4A5* in luminal (BT474, MCF-7, and T-47D) and basal (Hs578T, BT549, MDA-MB-157, and MDA-MB-231) breast cancer cell lines. (**E** and **F**) Western blot analysis (**E**) and relative protein level quantitation (**F**) of α5(IV) collagen protein levels in luminal (BT474, MCF-7, and T-47D) and basal (Hs578T, BT549, MDA-MB-157, and MDA-MB-231) breast cancer cell lines. (**G** and **H**) CCK-8 proliferation (**G**) and EdU incorporation (**H**) assays of MCF-7 and T-47D cells expressing scramble control shRNA or shRNA targeting *COL4A5* (CCK-8 assay, $n = 4$; EdU assay, $n = 3$). Data are presented as mean ± SEM. Statistical analyses were performed with two-tailed unpaired Student's *t*-test (**C**, **D**, and **F**), one-way ANOVA followed by Dunnett's multiple comparison test (**B** and **H**), or two-way ANOVA followed by Tukey's multiple comparison test (**G**). $^*P < 0.05$, $^{**}P < 0.01$, $^{***}P < 0.001$, $^{****}P < 0.0001$.

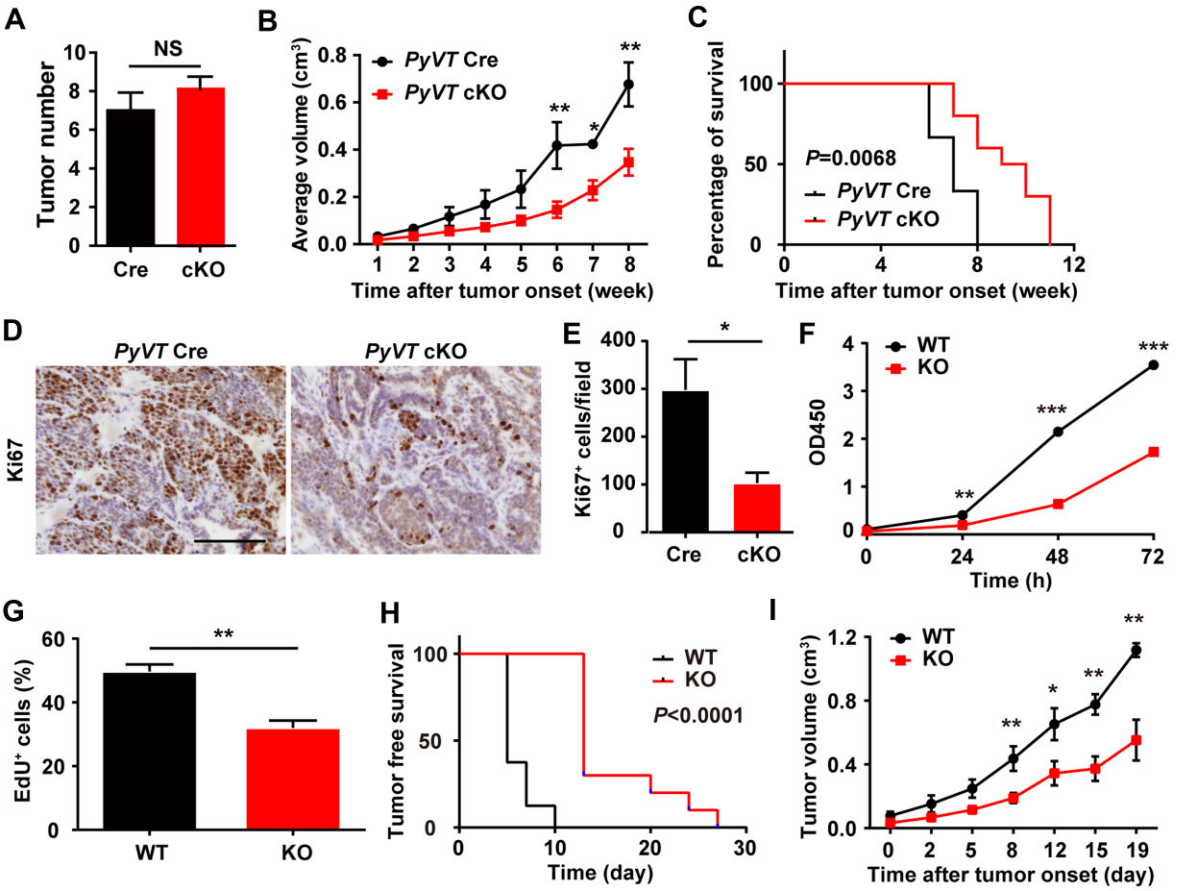

Figure 2 Ablation of α5(IV) in luminal mammary epithelial cells impairs *PyVT* tumor development. *MMTV-PyVT*;*Col4a5*$^{f/f}$;*Krt8-CreERT2* (cKO) and *MMTV-PyVT*;*Krt8-CreERT2* (Cre) mice were intraperitoneally injected with tamoxifen to induce luminal mammary epithelial cell-specific deletion of α5(IV). (**A**) Developed tumor numbers ($n = 6$ for Cre and $n = 10$ for cKO). (**B**) Kinetics of tumor growth after tumor onset ($n = 6$ for Cre and $n = 10$ for cKO). (**C**) Probabilities of survival after tumor onset ($n = 6$ for Cre and $n = 10$ for cKO). (**D** and **E**) Anti-Ki67 staining (**D**) and quantitation of Ki67-positive cell numbers (**E**) on *PyVT* tumor sections ($n = 3$). Scale bar, 100 μm. (**F** and **G**) CCK-8 proliferation (**F**) and EdU incorporation (**G**) assays of *PyVT* tumor cells ($n = 3$). (**H** and **I**) *PyVT* tumor cells were orthotopically injected into the fourth mammary fat pads of nude mice ($n = 8$ for WT and $n = 10$ for KO). (**H**) Tumor-free survival analysis. (**I**) Growth kinetics of xenograft tumors. Data are presented as mean ± SEM. Statistical analyses were performed with two-tailed unpaired Student's *t*-test (**A**, **E**, and **G**), two-way ANOVA followed by Tukey's multiple comparison test (**B**, **F**, and **I**), or log-rank test (**C** and **H**). NS, not significant. *$P < 0.05$, **$P < 0.01$, ***$P < 0.001$.

α5(IV) collagen is essential to breast cancer cell glycolysis

Gene set enrichment analysis (GSEA) of gene expression profiles of *PyVT* tumors revealed that signatures of E2F targets, G2/M checkpoint, and mitotic spindle assembly were the top negatively enriched gene signatures in KO *PyVT* tumors (Supplementary Figure S4A), consistent with the reduced tumor cell proliferation in KO *PyVT* tumors (Figure 2D and E). In addition to cell cycle regulation, glycolytic activity was significantly reduced in KO *PyVT* tumors (Figure 3A; Supplementary Figure S4A). Expression of glycolytic genes, including the glucose transporter *Slc2a1*/Glut1 and glycolytic enzymes PFKM, PFKP, GAPDH, and PGK1, was significantly reduced in KO *PyVT* tumors (Figure 3B–D) and KO *PyVT* cells (Figure 3E). Silencing α5(IV) collagen in MCF-7 and T-47D cells similarly reduced the expression of glucose transporter and glycolytic enzymes (Supplementary Figure S4B). Real-time measurement of tumor cell glycolytic rate using a Seahorse extracellular flux analyzer showed a much lower extracellular acidification rate (ECAR) of KO *PyVT* cells compared to WT *PyVT* cells (Figure 3F). KO *PyVT* cells had significantly lower glycolytic rate, total glycolytic capacity, and reserved glycolytic capacity (Figure 3G). As a result, KO *PyVT* cells had significantly less glucose consumption, lactate production, and adenosine triphosphate (ATP) production (Figure 3H–J). Silencing α5(IV) collagen significantly reduced glycolysis in MCF-7 and T-47D cells (Supplementary Figure S4C and D). Knockdown of ERα, the upstream regulator of α5(IV) collagen, similarly reduced glycolysis (Supplementary Figure S2D–F).

Normal cells rely primarily on mitochondrial oxidative phosphorylation to generate ATP. Cancer cells reprogram glucose metabolism and energy production from oxidative phosphorylation to glycolysis, known as the Warburg effect. We next examined whether α5(IV) collagen ablation would affect the balance

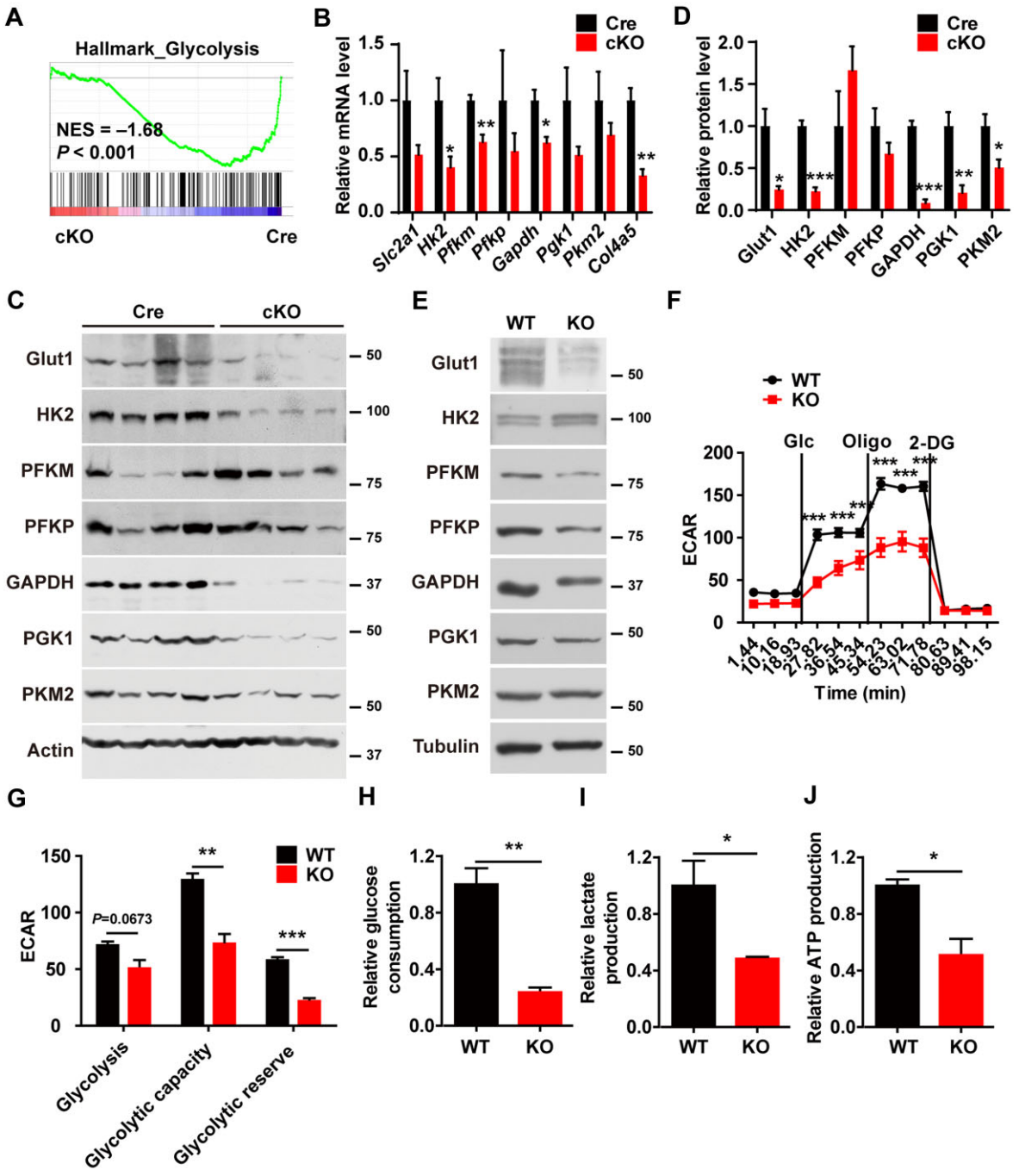

Figure 3 α5(IV) collagen regulates breast cancer glycolysis. (**A**) GSEA comparing enrichments of glycolysis signature genes in *PyVT* tumors. (**B**) The mRNA levels of glycolytic genes in *PyVT* tumors ($n = 4$). (**C** and **D**) Western blot analysis (**C**) and relative protein level quantitation (**D**) of glucose transporter and glycolytic enzymes in *PyVT* tumors ($n = 4$). (**E**) Western blot analysis of glucose transporter and glycolytic enzymes in *PyVT* tumor cells. (**F**) Real-time glycolytic rate measurement of *PyVT* tumor cells using a Seahorse extracellular flux analyzer ($n = 3$). (**G**) ECAR of *PyVT* tumor cells ($n = 3$). (**H**–**J**) Glucose consumption (**H**), lactate production (**I**), and ATP production (**J**) of *PyVT* tumor cells ($n = 3$). Data are presented as mean ± SEM. Statistical analyses were performed with two-tailed unpaired Student's *t*-test (**B**, **D**, **G**–**J**) or two-way ANOVA followed by Šídák's multiple comparison test (**F**). $^*P < 0.05$, $^{**}P < 0.01$, $^{***}P < 0.001$.

between glycolysis and oxidative phosphorylation. GSEA indicated that the oxidative phosphorylation pathway was not altered in KO *PyVT* tumors (Supplementary Figure S5A). Real-time measurement of tumor cell oxygen consumption rate revealed comparable basal respiration, ATP production from oxidative phosphorylation, maximal respiration, and spare respiratory capacity in α5(IV) collagen-ablated *PyVT*, MCF-7, and T-47D cells (Supplementary Figure S5B–D), suggesting that α5(IV) collagen mainly regulates glycolysis, but not oxidative phosphorylation in luminal breast cancer cells.

α5(IV) collagen regulates breast cancer cell glycolysis via DDR1 receptor

α5(IV) collagen ablation reduces the expression of the non-integrin collagen receptor DDR1 (Xiao et al., 2015). DDR1 is highly expressed in luminal breast cancer. α5(IV) collagen ablation resulted in reduced DDR1 expression in *PyVT* tumors (Figure 4A and B), *PyVT* cells (Figure 4C), and MCF-7 and T-47D cells (Figure 4D). Knockdown of ERα similarly reduced DDR1 expression (Supplementary Figure S2G). Silencing DDR1 expression in MCF-7 and T-47D cells significantly impaired cell proliferation (Figure 4E) and DNA synthesis (Figure 4F). Expression of the glucose transporter and glycolytic enzymes was significantly reduced in DDR1-knockdown breast cancer cells (Figure 4G). Real-time measurement of tumor cell glycolytic rate showed much lower ECAR of DDR1-knockdown MCF-7 and T-47D cells (Figure 4H) with significantly lower glycolytic rate, total glycolytic capacity, and reserved glycolytic capacity (Figure 4I). To further study whether DDR1 regulates the glycolysis downstream of α5(IV), constitutively active DDR1 (Div-DDR1) (Xiao et al., 2015) was expressed in α5(IV)-deficient *PyVT* cells. Ectopic Div-DDR1 expression restored the expression of the glucose transporter and glycolytic enzymes (Supplementary Figure S6A) and glycolytic activities (Supplementary Figure S6B and C) and thereafter restored the proliferation of α5(IV) collagen-ablated *PyVT* cells (Supplementary Figure S6D and E), indicating that α5(IV) collagen regulates breast cancer cell glycolysis through DDR1 receptor.

α5(IV) collagen regulates cancer cell glycolysis via c-Myc

Glycolysis has been shown to be associated with activated oncogenes (e.g. HIF and Myc) and mutant tumor suppressors (e.g. p53). GSEA indicated that Myc target genes were highly downregulated in KO *PyVT* tumors (Figure 5A). c-Myc expression was significantly reduced in KO *PyVT* tumors (Figure 5B and C), KO *PyVT* cells (Figure 5D), as well as in α5(IV) collagen-knockdown (Supplementary Figure S4B), DDR1-knockdown (Figure 4G), and ERα-knockdown (Supplementary Figure S2G) breast cancer cells, while its expression was restored in KO *PyVT* cells upon constitutively active DDR1 expression (Supplementary Figure S6A). Phosphorylation on Ser62 of c-Myc increases its transcriptional activity (Farrell and Sears, 2014). Phosphorylation level of c-Myc was significantly reduced in KO *PyVT* tumors (Figure 5B and C), KO *PyVT* cells (Figure 5D), and α5(IV) collagen-knockdown (Supplementary Figure S4B), DDR1-knockdown (Figure 4G), and ERα-knockdown (Supplementary Figure S2G) breast cancer cells. DDR1 triggers activation of the p38 MAPK pathway (Avivi-Green et al., 2006). c-Myc was predicted to be phosphorylated at Ser62 by p38 MAPK based on the sequence preferences of kinase catalytic domains (Linding et al., 2007). c-Myc and p38 MAPK were identified to interact with each other by a pairwise time-resolved fluorescence resonance energy transfer (TR-FRET)-based high-throughput screening of a cancer-focused protein–protein interaction network (OncoPPi) (Li et al., 2017). We next sought to investigate whether p38 MAPK is responsible for c-Myc phosphorylation downstream of α5(IV)–DDR1. α5(IV), DDR1, or ERα deficiency significantly reduced the phosphorylation levels of p38 MAPK (Figure 5E; Supplementary Figure S2G), which was restored upon constitutively active DDR1 expression (Supplementary Figure S6A). Treatment with the p38 MAPK-specific inhibitor SB203580 significantly reduced c-Myc phosphorylation and protein levels, glucose transporter and glycolytic enzyme expression (Figure 5F), and glycolytic activities (Figure 5G and H) in breast cancer cells.

To investigate whether the downregulated c-Myc expression is responsible for the reduced glycolysis in α5(IV) collagen-deficient breast cancer cells, c-Myc was ectopically expressed in KO *PyVT* cells. Re-expression of c-Myc restored the expression of the glucose transporter and glycolytic enzymes (Figure 6A and B). c-Myc restored not only Glut1 expression but also its proper plasma membrane localization (Figure 6B). Re-expression of c-Myc restored ECAR activity (Figure 6C), glycolytic rate, total glycolytic capacity, and reserved glycolytic capacity (Figure 6D) of KO *PyVT* cells. c-Myc-expressing KO *PyVT* cells had comparable glucose consumption, lactate production, and ATP production to WT *PyVT* cells (Figure 6E–G). Ectopic c-Myc expression partially restored cell proliferation and DNA synthesis of KO *PyVT* cells (Figure 6H and I), accelerated tumor onset to a level comparable to WT *PyVT* cells (Figure 6J), and partially restored tumor growth (Figure 6K–M).

α5(IV) collagen signature correlates with tumor glycolysis and predicts breast cancer prognosis

We next sought to investigate whether α5(IV) collagen indeed regulates the c-Myc–glycolysis axis in breast cancer patients. Consistent with previous reports, c-Myc target gene expression (Myc signature) highly correlated with glycolytic activity (glycolysis signature) in the NKI cohort (Figure 7A). α5(IV) collagen KO *PyVT* tumors had a distinct gene expression pattern from WT tumors. Differentially expressed genes in KO *PyVT* tumors were used as α5(IV) collagen signature (Col4a5 collagen signature). Col4a5 collagen signature significantly correlated with glycolytic activity and c-Myc target gene expression in the NKI cohort (Figure 7B and C). Cox analyses were performed to determine whether the clinical outcome of breast cancer patients could be predicted by the expression of α5(IV) collagen. Cox analyses indicated that Col4a5 collagen signature ($\chi^2 = 18.286$; $P < 0.0001$), Myc signature ($\chi^2 = 17.189$; $P < 0.0001$), and glycolysis signature ($\chi^2 = 24.362$; $P < 0.0001$) were predictive

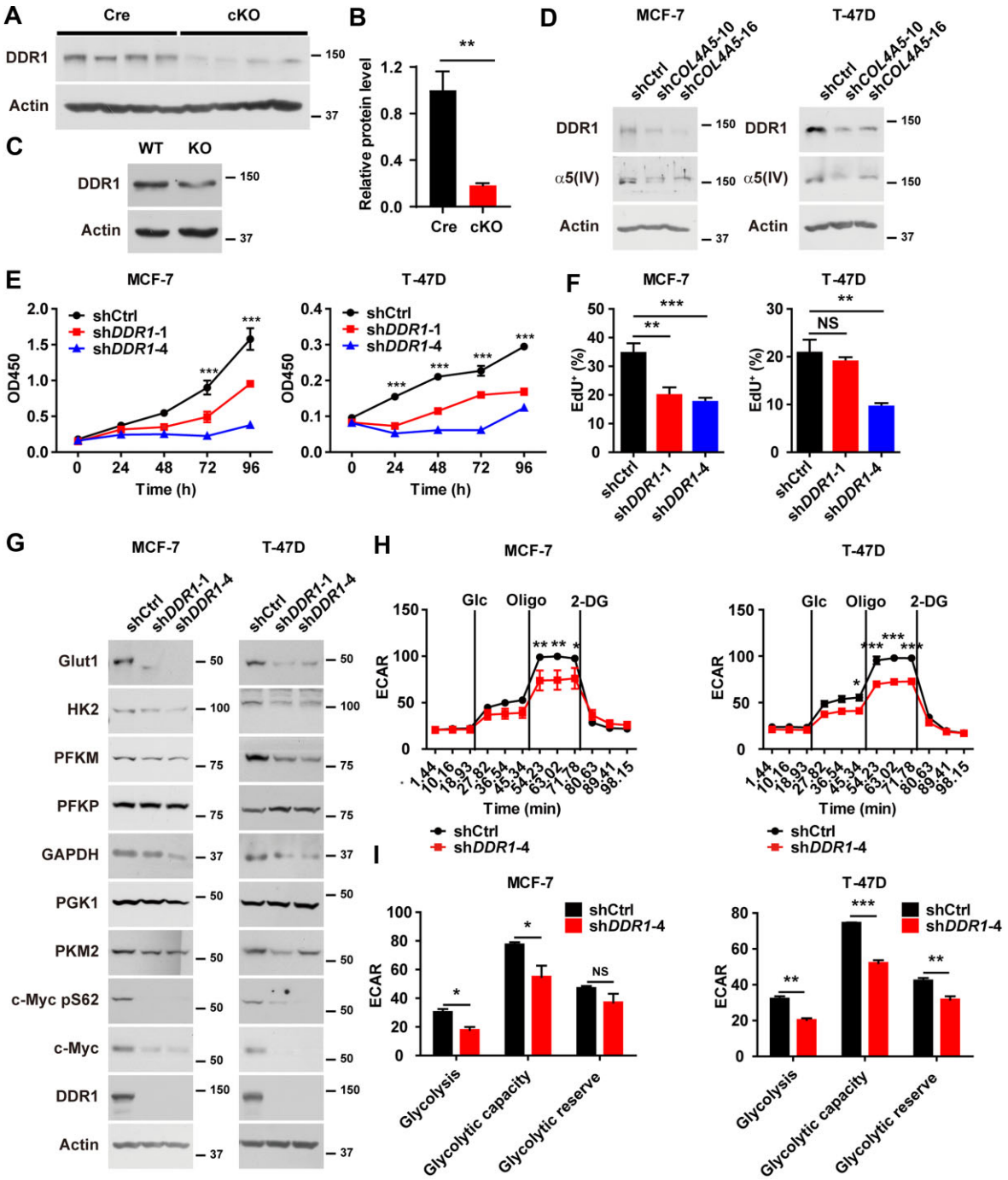

Figure 4 DDR1 regulates breast cancer glycolysis and proliferation. (**A** and **B**) Western blot analysis (**A**) and relative protein level quantitation (**B**) of DDR1 in *PyVT* tumors ($n = 4$). (**C**) Western blot analysis of DDR1 in *PyVT* tumor cells. (**D**) Western blot analysis of DDR1 in α5(IV) collagen-knockdown MCF-7 and T-47D cells. (**E** and **F**) CCK-8 proliferation (**E**) and EdU incorporation (**F**) assays of control and DDR1-knockdown MCF-7 and T-47D cells ($n = 3$). (**G**) Western blot analysis of c-Myc, glucose transporter, and glycolytic enzymes in control and DDR1-knockdown MCF-7 and T-47D cells. (**H**) Real-time glycolytic rate measurement of control and DDR1-knockdown MCF-7 and T-47D cells ($n = 3$). (**I**) ECAR of control and DDR1-knockdown MCF-7 and T-47D cells ($n = 3$). Data are presented as mean ± SEM. Statistical analyses were performed with two-tailed unpaired Student's *t*-test (**B** and **I**), one-way ANOVA followed by Dunnett's multiple comparison test (**F**), or two-way ANOVA followed by Tukey's (**E**) or Šídák's (**H**) multiple comparison test. $^*P < 0.05$, $^{**}P < 0.01$, $^{***}P < 0.001$. NS, not significant.

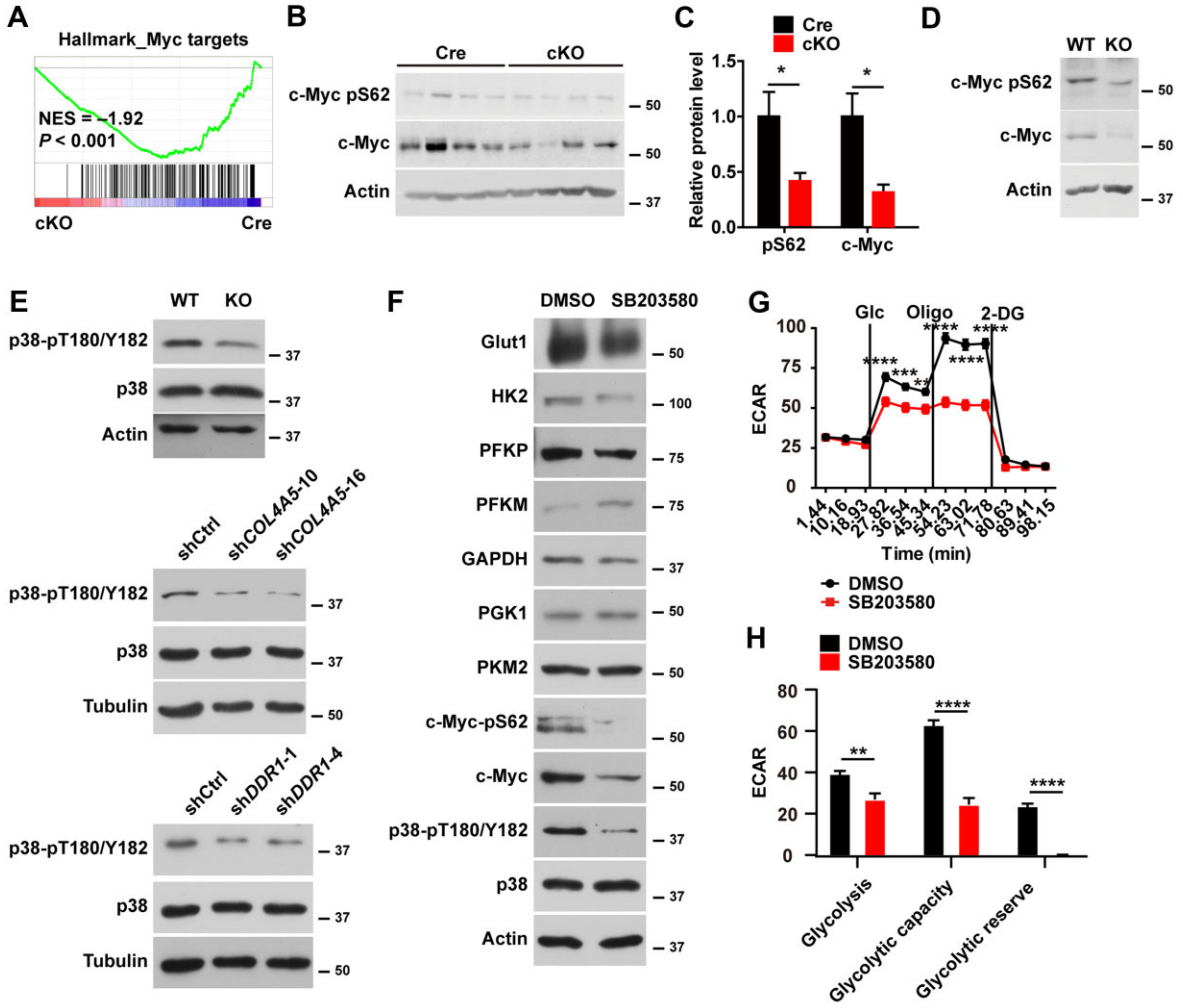

Figure 5 α5(IV) collagen regulates breast cancer glycolysis via c-Myc. (**A**) GSEA comparing enrichments of c-Myc target genes in *PyVT* tumors. (**B** and **C**) Western blot analysis (**B**) and quantification (**C**) of c-Myc protein and Ser62 phosphorylation levels in *PyVT* tumors ($n = 4$). (**D**) Western blot analysis of c-Myc protein and Ser62 phosphorylation levels in *PyVT* tumor cells. (**E**) Western blot analysis of p38 MAPK phosphorylation levels in *PyVT* tumor cells and MCF-7 cells deficient of α5(IV) or DDR1. (**F**) Western blot analysis of c-Myc, glucose transporter, and glycolytic enzyme levels in *PyVT* tumor cells subjected to p38 MAPK inhibitor SB203580 treatment. (**G**) Real-time glycolytic rate measurement of *PyVT* tumor cells subjected to p38 MAPK inhibitor SB203580 treatment ($n = 10$). (**H**) ECAR of *PyVT* tumor cells subjected to p38 MAPK inhibitor SB203580 treatment ($n = 10$). Data are presented as mean ± SEM. Statistical analyses were performed with two-tailed unpaired Student's *t*-test (**C** and **H**) or two-way ANOVA followed by Šídák's multiple comparison test (**G**). $^{*}P < 0.05$, $^{**}P < 0.01$, $^{***}P < 0.001$, $^{****}P < 0.0001$.

for the overall survival of breast cancer patients. Breast cancer patients with high glycolytic activity (HR: 3.24 (2.07–5.09); $P < 0.0001$) (Figure 7D) or high Myc target gene expression (HR: 2.50 (1.60–3.90); $P = 0.0001$) (Figure 7E) had significantly shorter survival time. Consistently, patients with a high Col4a5 collagen signature had a significantly shorter survival time (HR: 5.16 (2.80–9.52); $P < 0.0001$) (Figure 7F). These data collectively suggest that α5(IV) collagen regulates tumor glycolysis and could predict breast cancer prognosis.

Discussion

Breast cancer subtypes exhibit diverse clinical features and clinical outcomes, which are determined not only by subtype-specific gene expression but also by the interaction with the heterogeneous tumor microenvironment. ECM is the major non-cellular component in the tumor microenvironment. ECM compositions are significantly different in normal and diseased tissues (Lai et al., 2011; Naba et al., 2012, 2017; Schiller et al., 2015; Gocheva et al., 2017; Massey et al., 2017; Bergmeier et al., 2018; Yuzhalin et al., 2018; Martin et al., 2020; Wu et al., 2021). Interestingly, type IV collagen α chains are differentially expressed in different breast cancer subtypes, i.e. α5(IV) is preferentially expressed in luminal A/normal breast-like subtypes, whereas α1(IV)/α2(IV) is more abundantly expressed in basal-like/ERBB2/luminal B subtypes. Type IV collagens are the core components forming the framework of BMs

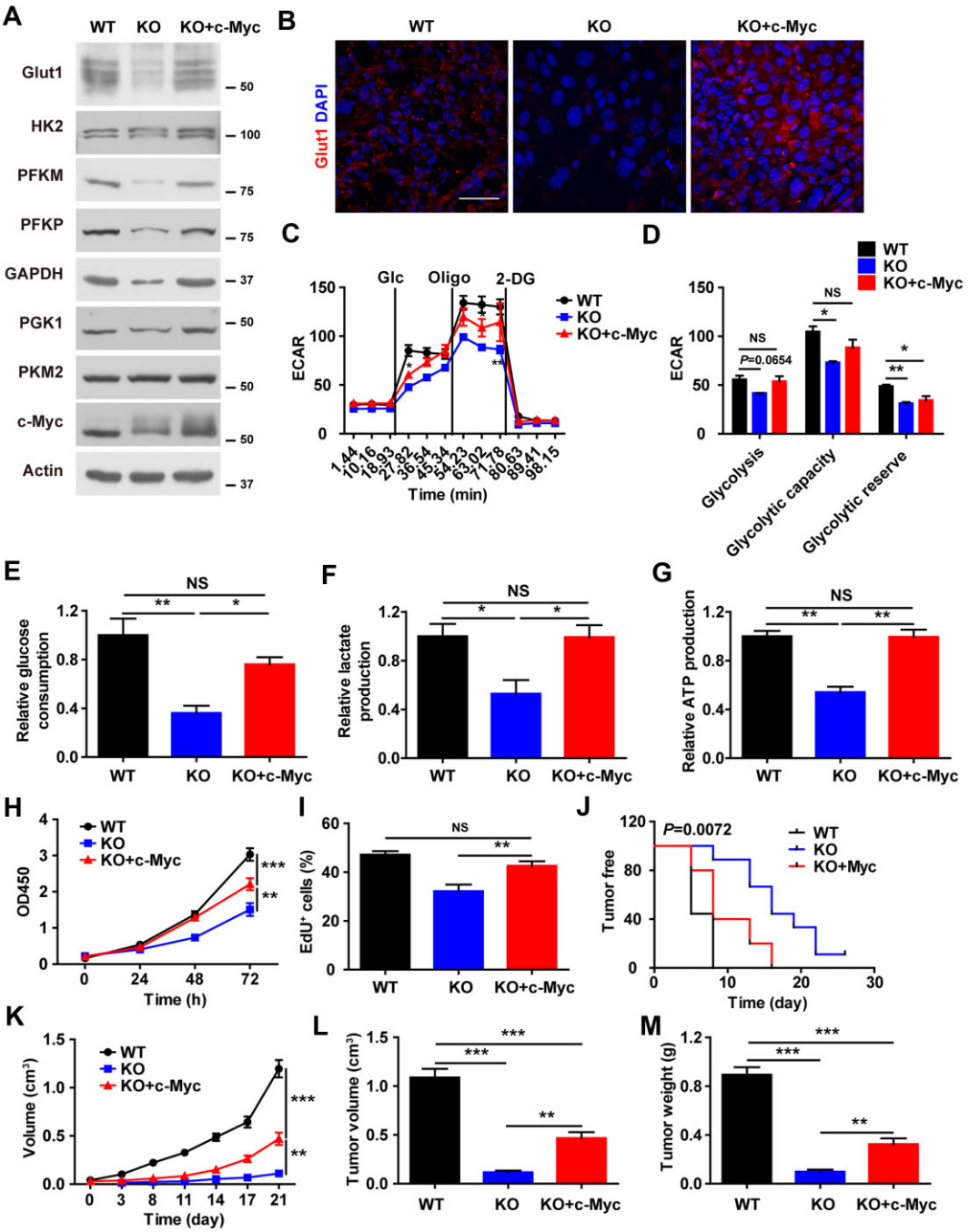

Figure 6 c-Myc partially restores α5(IV) collagen-deficient cancer cell proliferation and tumorigenicity. (**A**) Western blot analysis of glucose transporter and glycolytic enzyme levels in *PyVT* tumor cells ectopically expressing c-Myc. (**B**) Immunofluorescent staining of the Glut1 transporter in *PyVT* tumor cells ectopically expressing c-Myc. Scale bar, 100 μm. (**C**) Real-time glycolytic rate measurement of c-Myc-expressing *PyVT* tumor cells using a Seahorse extracellular flux analyzer ($n = 3$). (**D**) ECAR of c-Myc-expressing *PyVT* tumor cells ($n = 3$). (**E**–**G**) Glucose consumption (**E**), lactate production (**F**), and ATP production (**G**) of c-Myc-expressing *PyVT* tumor cells ($n = 3$). (**H** and **I**) CCK-8 proliferation (**H**) and EdU incorporation (**I**) assays of c-Myc-expressing *PyVT* tumor cells ($n = 3$). (**J**–**M**) *PyVT* tumor cells were orthotopically injected into the fourth mammary fat pads of nude mice ($n = 9$ for WT, $n = 9$ for KO, and $n = 10$ for c-Myc-expressing KO cells). (**J**) Tumor-free survival analysis. (**K**) Growth kinetics of xenograft tumors. (**L** and **M**) Tumor volume and tumor weight of xenograft tumors. Data are presented as mean ± SEM. Statistical analyses were performed with one-way ANOVA followed by Dunnett's multiple comparison test (**D**–**G**, **I**, **L**, and **M**), two-way ANOVA followed by Šídák's (**C**) or Tukey's (**H** and **K**) multiple comparison test, or log-rank test (**J**). $^*P < 0.05$, $^{**}P < 0.01$, $^{***}P < 0.001$. NS, not significant.

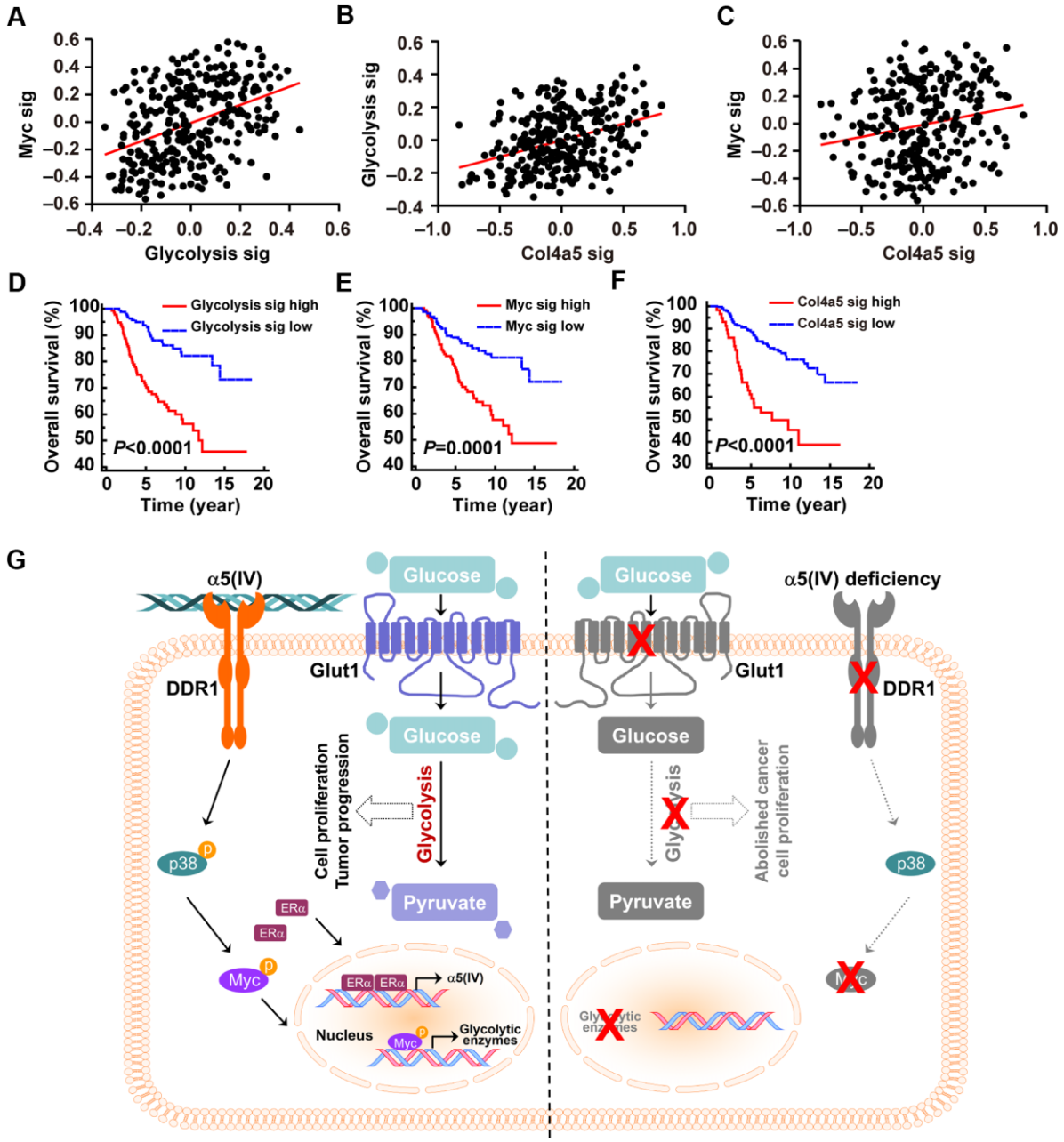

Figure 7 α5(IV) collagen highly correlates with glycolysis and c-Myc in breast cancer tumors. GSVA scores of differentially expressed genes in α5(IV) collagen-deficient tumors (Col4a5 signature), glycolytic genes (glycolysis signature), and c-Myc target genes (Myc signature) were calculated for each breast cancer patient sample in the NKI cohort. (**A**–**C**) Col4a5 signature, glycolysis signature, and Myc signature positively correlate to each other in the NKI cohort. (**D**–**F**) Probabilities of survival of breast cancer patients according to the expression level of the glycolysis (**D**), Myc (**E**), and Col4a5 (**F**) signatures. Statistical analyses were performed with log-rank test. (**G**) Diagram illustration of the regulation of α5(IV) collagen–DDR1–p38 MAPK–c-Myc signaling axis on luminal breast cancer glycolysis.

(Kalluri, 2003; Pozzi et al., 2017). The preference of α5(IV) expression in ERα-positive luminal breast cancer and the differential composition of BM proteins in breast cancer subtypes suggest that α5(IV) collagen may play essential roles in supporting this particular breast cancer subtype that cannot be substituted by α1(IV)/α2(IV) collagens. Indeed, deficiency of α5(IV) collagen significantly impairs luminal breast cancer cell proliferation and tumor development.

Cancer cells reprogram their metabolism to meet the demand for rapid growth. Cancer cells primarily supply energy through glycolysis, even in aerobic conditions. Cancer cell glycolysis is regulated by the tumor microenvironment. The low-oxygen

tension and cytokines secreted by stromal cells are important microenvironmental regulators of tumor glycolysis (Denko, 2008; Li et al., 2018; Zhang et al., 2018; Bertero et al., 2019). Besides hypoxia and cytokines, α5(IV) collagen is essential to maintain the expression of glucose transporters and glycolytic enzymes in luminal breast cancer cells. Depletion of α5(IV) collagen drastically reduces glycolysis capability and proliferation of luminal breast cancer cells. Thus, α5(IV) collagen represents another class of microenvironmental regulators of tumor glycolysis. ER-stimulated glycolysis is at least in part regulated by the interaction between luminal breast cancer cells and α5(IV) collagen in their subtype-specific microenvironment.

c-Myc is one of the key regulators driving the expression of glycolytic enzymes and augmenting the Warburg effect (Hsieh et al., 2015). α5(IV) collagen is essential to maintain c-Myc phosphorylation and protein levels and thus glycolytic activity in luminal breast cancer cells, in part by regulating p38 MAPK kinase activation via DDR1. It warrants further investigation whether c-Myc phosphorylation is directly mediated by p38 MAPK or is an indirect effect of p38 MAPK activation and cell proliferation status. Nevertheless, the non-integrin receptor DDR1 and its downstream kinase p38 MAPK are essential to maintain c-Myc expression and phosphorylation in luminal-type breast cancer cells and for the pro-tumoral effects of α5(IV) collagen (Figure 7G). Such regulation axis is not only observed in breast cancer cells and tumor models but also reflected in clinical samples. Despite restoration of c-Myc expression fully restores glycolysis and *in vitro* proliferation of α5(IV) collagen-deficient luminal breast cancer cells, c-Myc expression only partially restores tumor growth *in vivo*, suggesting that other signaling pathways downstream of α5(IV) collagen, in synergy with the DDR1–p38 MAPK–c-Myc–glycolysis signaling, are involved in regulating tumor development *in vivo*.

In summary, α5(IV) is preferentially expressed in luminal-type breast cancer and is essential for luminal-type breast cancer cell proliferation and tumor development through the DDR1–p38 MAPK–c-Myc signaling axis-driven aerobic glycolysis. α5(IV) is thus an important tumor microenvironmental factor in regulating luminal-type breast cancer metabolism.

Materials and methods

Mouse treatment

Knockout-first *Col4a5*$^{LacZ/+}$ (European Conditional Mouse Mutagenesis Program) mice (Xiao et al., 2015) were crossed with *Flper* mice (Jackson Laboratory) to generate the *Col4a5*$^{f/+}$ mice. *Col4a5*$^{f/+}$ mice were maintained in C57/BL6 background. *Krt8-CreERT2* mice (Zhang et al., 2012) were generously provided by Prof. Li Xin at the University of Washington. Tg(*MMTV-PyVT*)634Mul/J mice were from Jackson Laboratory. All mice were housed in a specific pathogen-free environment at the Shanghai Institute of Biochemistry and Cell Biology (SIBCB) and treated in strict accordance with protocols approved by the Institutional Animal Care and Use Committee of SIBCB (approval number: SIBCB-NAF-15-003-S325-006).

Three-week-old *MMTV-PyVT*;*Col4a5*$^{f/f}$;*Krt8-CreERT2* (cKO) and *MMTV-PyVT*;*Krt8-CreERT2* (Cre) mice were intraperitoneally injected with 160 μg/g body weight tamoxifen (Sigma) twice a week for three times to induce *Col4a5* exon 36 deletion and reading frame shift in luminal mammary epithelial cells. Tumor development was monitored every week. A total of 5×10^4 *PyVT* tumor cells suspended in 100 μl 50% growth factor reduced Matrigel (BD, 356231) were orthotopically injected into the fourth mammary fat pads of 7-week-old female nude mice (Shanghai SLAC Laboratory Animal Co.). Tumor development was monitored twice a week. Tumor samples were fixed in 4% paraformaldehyde and processed for paraffin embedding. Paraffin-embedded tissues were sectioned and stained with hematoxylin and eosin or subjected to immunohistochemistry.

Cell lines

MCF-7 breast cancer cells (ATCC) were maintained in DMEM (Gibco) supplemented with 10% fetal bovine serum (FBS) (Ausbian) and 10 μg/ml insulin (Sigma). T-47D breast cancer cells (ATCC) were maintained in RPMI 1640 (Gibco) supplemented with 10% FBS and 10 μg/ml insulin. 293T cells (ATCC) were maintained in DMEM supplemented with 10% FBS. Primary tumor cells were isolated from WT or KO *PyVT* mice and immortalized with hTERT. Immortalized *PyVT* tumor cells were cultured in DMEM supplemented with 10% FBS and 50 μg/ml hygromycin (Amresco). shRNAs were cloned into pLKO.1-puro lentiviral vector (Addgene). The target sequences are listed in Supplementary Table S1. After viral infection, cells were selected with puromycin (Gibco) to generate stable cell lines. c-Myc was cloned into pBabe-neo retroviral vector (Addgene). Cells were selected with neomycin (Gibco) to generate stable cell lines. At least two batches of stable cell lines were generated for each experiment. All cell lines were routinely tested for mycoplasma contamination. Experiments were performed in triplicate and repeated at least twice. Cell Counting Kit-8 (CCK8) (Dojindo) and EdU (Beyotime Biotechnology) incorporation assays were performed according to the manufacturer's protocol.

Glucose consumption and lactate production

PyVT tumor cells (2×10^5) were seeded in a 12-well plate, and the medium was changed after 6 h. After 24 h, the medium was collected. Glucose consumption (Glucose Assay Kit, Sigma) and lactate production (Lactate Colorimetric/Fluorometric Assay Kit, Biovision) were measured according to the manufacturer's protocol.

ATP production

PyVT tumor cells (3×10^3) were seeded in a 96-well plate, and the medium was changed after 6 h. The medium was collected after 24 h. ATP production (CellTiter-Glo Luminescent Cell Viability Assay, Promega) was measured according to the manufacturer's protocol.

ECAR and oxygen consumption rate

Approximately 5×10^4 to 8×10^4 cells were seeded in the XF24 plate, and 150 μl of growth medium was added to each well after 6 h. Cells were cultured overnight. Cells were washed and cultured in a 37°C incubator without CO_2 for 1 h prior to the assay. For ECAR measurement, stock compounds from the XF Glycolysis Stress Test Kit were diluted into the XF Glycolysis Stress Test assay medium and loaded into the cartridge ports to achieve final concentrations of 10 mM glucose, 2 μM oligomycin, and 100 mM 2-deoxy-D-glucose. For oxygen consumption rate measurement, stock compounds from the XF Cell Mito Stress Test Kit were diluted into XF Cell Mito Stress Test assay medium and loaded into the cartridge ports to achieve final concentrations of 1 μM oligomycin, 0.5 μM FCCP, and 1 μM antimycin/rotenone.

Western blot and quantitative real-time PCR (qRT-PCR) analyses

Tumors were homogenated in sodium dodecyl sulfate sample buffer or Trizol reagents (Invitrogen). Western blot and qRT-PCR analyses were performed as previously described (Gao et al., 2010). The primary antibodies and primers used are listed in Supplementary Tables S2 and S3, respectively. Gene expression levels were normalized to actin. All experiments were performed at least twice.

Immunohistochemistry and immunocytochemistry staining

Immunohistochemistry on 5-μm paraffin tumor sections using antibody against Ki-67 (Novocastra Laboratories) was performed according to the manufacturer's instructions. *PyVT* tumor cells (1×10^5) were plated on glass coverslips and grew overnight. Cells were fixed with 4% paraformaldehyde and permeabilized with 0.15% Triton X-100. Cells were blocked with 3% bovine serum albumin for 2 h at room temperature and then incubated with Glut1 primary antibody (Abcam, ab40084) at 4°C overnight. Cells were stained with Alexa Fluor 555-conjugated secondary antibody for 1 h at room temperature and counterstained with 4′,6-diamidino-2-phenylindole (DAPI). Images were captured with confocal laser scanning microscopy (Leica).

RNA sequencing analyses

Total RNA was extracted and purified from tumors using Trizol (Invitrogen). Three biological replicates were subjected to complementary DNA library preparation according to the Illumina standard protocol. Libraries were sequenced on the NovaSeq 6000 with 150-bp paired-end sequencing (Berry Genomics). After cutting adapters by Trimgalore (v.0.5.0), RNA sequencing data were mapped to the mouse mm10 reference genome by STAR (v.2.9). FeatureCount in Subread package (v.1.6.4) was used to count reads. R package DESeq2 (v.1.24.0) was used to perform normalization and differential expression analysis. Gene set variation analysis (GSVA) was run on default parameters using R package GSVA (v.1.32.0) (Hanzelmann et al., 2013). GSEA was performed on gene signatures obtained from the MSigDB database v5.0 (March 2015 release) (Subramanian et al., 2005). Statistical significance of GSEA analysis was assessed by comparing the enrichment score to enrichment results generated from 1000 random permutations of the gene set to obtain *P*-values (nominal *P*-value). Survival analysis was performed on previously published breast cancer microarray datasets (NKI and GSE25066) (van de Vijver et al., 2002; Hatzis et al., 2011) using the uni-variable and multi-variable Cox regression and Kaplan–Meier (log-rank test) method.

Statistical analysis

Statistical analyses were performed with two-tailed unpaired Student's *t*-test, one-way analysis of variance (ANOVA) followed by Dunnett's multiple comparison test, two-way ANOVA followed by Tukey's or Šídák's multiple comparison test, or log-rank test. All error bars represent standard error of the mean (SEM).

Supplementary material

Supplementary material is available at *Journal of Molecular Cell Biology* online.

Acknowledgements

The authors acknowledge Prof. Li Xin (University of Washington) for sharing mouse model, Prof. Weiwei Yang (SIBCB) for helpful discussion, and Drs Baojin Wu and Guoyuan Chen for technical support.

Funding

This work was supported by grants from the Ministry of Science and Technology of China (2020YFA0803203) and the National Natural Science Foundation of China (81430067, 32070789, and 31900514).

Conflict of interest: none declared.

Author contributions: Y.W. and X.L.: study design, acquisition, analysis, and interpretation of data, and assistance in manuscript preparation. Y.Z., Y.Q., and Y.G.: acquisition of data. Y.W., X.L., Y.G., and J.C.: interpretation of data and assistance in manuscript preparation. G.G.: study concept and design, interpretation of data, study supervision, and manuscript preparation.

References

Avivi-Green, C., Singal, M., and Vogel, W.F. (2006). Discoidin domain receptor 1-deficient mice are resistant to bleomycin-induced lung fibrosis. Am. J. Respir. Crit. Care Med. *174*, 420–427.

Bergmeier, V., Etich, J., Pitzler, L., et al. (2018). Identification of a myofibroblast-specific expression signature in skin wounds. Matrix Biol. *65*, 59–74.

Bertero, T., Oldham, W.M., Grasset, E.M., et al. (2019). Tumor–stroma mechanics coordinate amino acid availability to sustain tumor growth and malignancy. Cell Metab. *29*, 124–140.e10.

Borza, D.B., Bondar, O., Ninomiya, Y., et al. (2001). The NC1 domain of collagen IV encodes a novel network composed of the α1, α2, α5, and α6 chains in smooth muscle basement membranes. J. Biol. Chem. *276*, 28532–28540.

Boutaud, A., Borza, D.B., Bondar, O., et al. (2000). Type IV collagen of the glomerular basement membrane. Evidence that the chain specificity of

network assembly is encoded by the noncollagenous NC1 domains. J. Biol. Chem. *275*, 30716–30724.

Butkowski, R.J., Wieslander, J., Kleppel, M., et al. (1989). Basement membrane collagen in the kidney: regional localization of novel chains related to collagen IV. Kidney Int. *35*, 1195–1202.

Denko, N.C. (2008). Hypoxia, HIF1 and glucose metabolism in the solid tumour. Nat. Rev. Cancer *8*, 705–713.

Farrell, A.S., and Sears, R.C. (2014). MYC degradation. Cold Spring Harb. Perspect. Med. *4*, a014365.

Gao, Y., Xiao, Q., Ma, H., et al. (2010). LKB1 inhibits lung cancer progression through lysyl oxidase and extracellular matrix remodeling. Proc. Natl Acad. Sci. USA *107*, 18892–18897.

Gocheva, V., Naba, A., Bhutkar, A., et al. (2017). Quantitative proteomics identify Tenascin-C as a promoter of lung cancer progression and contributor to a signature prognostic of patient survival. Proc. Natl Acad. Sci. USA *114*, E5625–E5634.

Gunwar, S., Ballester, F., Noelken, M.E., et al. (1998). Glomerular basement membrane. Identification of a novel disulfide-cross-linked network of α3, α4, and α5 chains of type IV collagen and its implications for the pathogenesis of Alport syndrome. J. Biol. Chem. *273*, 8767–8775.

Hanahan, D., and Weinberg, R.A. (2011). Hallmarks of cancer: the next generation. Cell *144*, 646–674.

Hanzelmann, S., Castelo, R., and Guinney, J. (2013). GSVA: gene set variation analysis for microarray and RNA-seq data. BMC Bioinf. *14*, 7.

Hatzis, C., Pusztai, L., Valero, V., et al. (2011). A genomic predictor of response and survival following taxane–anthracycline chemotherapy for invasive breast cancer. JAMA *305*, 1873–1881.

Hsieh, A.L., Walton, Z.E., Altman, B.J., et al. (2015). MYC and metabolism on the path to cancer. Semin. Cell Dev. Biol. *43*, 11–21.

Hynes, R.O., and Naba, A. (2012). Overview of the matrisome—an inventory of extracellular matrix constituents and functions. Cold Spring Harb. Perspect. Biol. *4*, a004903.

Kalluri, R. (2003). Basement membranes: structure, assembly and role in tumour angiogenesis. Nat. Rev. Cancer *3*, 422–433.

Lai, K.K., Shang, S., Lohia, N., et al. (2011). Extracellular matrix dynamics in hepatocarcinogenesis: a comparative proteomics study of PDGFC transgenic and Pten null mouse models. PLoS Genet. *7*, e1002147.

Li, W., Tanikawa, T., Kryczek, I., et al. (2018). Aerobic glycolysis controls myeloid-derived suppressor cells and tumor immunity via a specific CEBPB isoform in triple-negative breast cancer. Cell Metab. *28*, 87–103.e6.

Li, Z., Ivanov, A.A., Su, R., et al. (2017). The OncoPPi network of cancer-focused protein–protein interactions to inform biological insights and therapeutic strategies. Nat. Commun. *8*, 14356.

Linding, R., Jensen, L.J., Ostheimer, G.J., et al. (2007). Systematic discovery of in vivo phosphorylation networks. Cell *129*, 1415–1426.

Liu, J., Zhang, C., Hu, W., et al. (2019). Tumor suppressor p53 and metabolism. J. Mol. Cell Biol. *11*, 284–292.

Martin, D.R., Witten, J.C., Tan, C.D., et al. (2020). Proteomics identifies a convergent innate response to infective endocarditis and extensive proteolysis in vegetation components. JCI Insight *5*, e135317.

Massey, V.L., Dolin, C.E., Poole, L.G., et al. (2017). The hepatic 'matrisome' responds dynamically to injury: characterization of transitional changes to the extracellular matrix in mice. Hepatology *65*, 969–982.

Naba, A., Clauser, K.R., Hoersch, S., et al. (2012). The matrisome: in silico definition and in vivo characterization by proteomics of normal and tumor extracellular matrices. Mol. Cell. Proteomics *11*, M111.014647.

Naba, A., Pearce, O.M.T., Del Rosario, A., et al. (2017). Characterization of the extracellular matrix of normal and diseased tissues using proteomics. J. Proteome Res. *16*, 3083–3091.

Pietras, K., and Ostman, A. (2010). Hallmarks of cancer: interactions with the tumor stroma. Exp. Cell Res. *316*, 1324–1331.

Poschl, E., Schlotzer-Schrehardt, U., Brachvogel, B., et al. (2004). Collagen IV is essential for basement membrane stability but dispensable for initiation of its assembly during early development. Development *131*, 1619–1628.

Pozzi, A., Yurchenco, P.D., and Iozzo, R.V. (2017). The nature and biology of basement membranes. Matrix Biol. *57–58*, 1–11.

Randles, M.J., Humphries, M.J., and Lennon, R. (2017). Proteomic definitions of basement membrane composition in health and disease. Matrix Biol. *57–58*, 12–28.

Schiller, H.B., Fernandez, I.E., Burgstaller, G., et al. (2015). Time- and compartment-resolved proteome profiling of the extracellular niche in lung injury and repair. Mol. Syst. Biol. *11*, 819.

Subramanian, A., Tamayo, P., Mootha, V.K., et al. (2005). Gene set enrichment analysis: a knowledge-based approach for interpreting genome-wide expression profiles. Proc. Natl Acad. Sci. USA *102*, 15545–15550.

van de Vijver, M.J., He, Y.D., van't Veer, L.J., et al. (2002). A gene-expression signature as a predictor of survival in breast cancer. N. Engl. J. Med. *347*, 1999–2009.

Ward, P.S., and Thompson, C.B. (2012). Metabolic reprogramming: a cancer hallmark even Warburg did not anticipate. Cancer Cell *21*, 297–308.

Wu, Y., Cao, Y., Xu, K., et al. (2021). Dynamically remodeled hepatic extracellular matrix predicts prognosis of early-stage cirrhosis. Cell Death Dis. *12*, 163.

Wu, Y., and Ge, G. (2019). Complexity of type IV collagens: from network assembly to function. Biol. Chem. *400*, 565–574.

Xiao, Q., Jiang, Y., Liu, Q., et al. (2015). Minor type IV collagen α5 chain promotes cancer progression through discoidin domain receptor-1. PLoS Genet. *11*, e1005249.

Yuzhalin, A.E., Urbonas, T., Silva, M.A., et al. (2018). A core matrisome gene signature predicts cancer outcome. Br. J. Cancer *118*, 435–440.

Zhang, L., Zhang, B., Han, S.J., et al. (2012). Targeting CreER^{T2} expression to keratin 8-expressing murine simple epithelia using bacterial artificial chromosome transgenesis. Transgenic Res. *21*, 1117–1123.

Zhang, Y., Yu, G., Chu, H., et al. (2018). Macrophage-associated PGK1 phosphorylation promotes aerobic glycolysis and tumorigenesis. Mol. Cell *71*, 201–215.e7.

Zhou, J., Ding, M., Zhao, Z., et al. (1994). Complete primary structure of the sixth chain of human basement membrane collagen, α6(IV). Isolation of the cDNAs for α6(IV) and comparison with five other type IV collagen chains. J. Biol. Chem. *269*, 13193–13199.